The CMS Pixel Tracking Telescope at the Fermilab Test Beam Facility

Simon Kwan$_a$, CM Lei$_a$, Dario Menasce$_b$, Luigi Moroni$_b$, Jennifer Ngadiuba$_b$, Alan Prosser$_a$, Ryan Rivera$_a$, Stefano Terzo$_b$, Marcos Turqueti[1]$_a$, Lorenzo Uplegger$_a$, Luigi Vigani$_b$

a Fermi National Accelerator Laboratory, Batavia, IL, USA

b Istituto Nazionale di Fisica Nucleare, Sezione di Milano Bicocca, and Università degli Studi di Milano Bicocca, Piazza della Scienza 3, 20126 Milano, Italy

E-mail: uplegger@fnal.gov

Abstract

An all silicon pixel telescope has been assembled and used at the Fermilab Test Beam Facility (FTBF) for the last four years to provide precise tracking information for different test beam experiments with a wide range of Detectors Under Test (DUTs) requiring high resolution measurement of the track impact point. The telescope is based on CMS pixel modules left over from the CMS forward pixel production. Eight planes are arranged to achieve a resolution of less than 6 μm on the beam transverse coordinate at the DUT position. In order to achieve such resolution with 100 x 150 μm^2 pixel cells, the planes were tilted to 25 degrees to maximize charge sharing between pixels. Crucial for obtaining this performance is the alignment software, called Monicelli, specifically designed and optimized for this system. This paper will describe the telescope hardware, the data acquisition system and the alignment software constituting this particle tracking system for test beam users.

1 Introduction

The Fermilab Test Beam Facility (FTBF) at the Fermi National Accelerator Laboratory provides beam in a multitude of particle types and a range of energies with which users can test their detectors [1]. The beam is resonantly extracted in a slow spill for each Main Injector cycle delivering a single 4.2 second long spill per minute. The primary beam consists of high energy protons (120 GeV) at variable intensities between 1 and 300 KHz. This beam can also be targeted to create secondary particle beams of pions, muons or electrons with energies down to about 1 GeV. Users have access to the facility instrumentation to measure the position and energy of the incident beam. Four pre-installed scintillation counters give rough beam position, a lead glass calorimeters measure the beam energy to a precision of ~3%, two time of flight detectors can be set up for particle identification, and finally a silicon pixel telescope provides a precision position measurement of less than 6 μm. The silicon pixel telescope will be described in this paper along with its data

[1] *Now at Lawrence Berkeley National Laboratory, Berkeley, CA, USA*

Operated by Fermi Research Alliance, LLC under Contract No. De-AC02-07CH11359 with the United States Department of Energy.

acquisition (DAQ) system and alignment software.

2 The Pixel Telescope

A CMS pixel-based telescope has been built to provide precision tracking information to any test beam experiment at the FTBF in need of knowing the particle impact point on their detector under tests (DUTs) with accurate precision. The telescope is placed along the FTBF beam line and consists of eight detector planes - each made of modules left over from the CMS Forward Pixel detector production - mounted on a carbon fiber frame. Four of the eight telescope planes use modules composed of six (2x3) PSI46V2 Read Out Chips (ROCs) [2], while the remaining four planes are equipped with 2x4 modules. One of the 2x4 modules is shown in Figure 1.

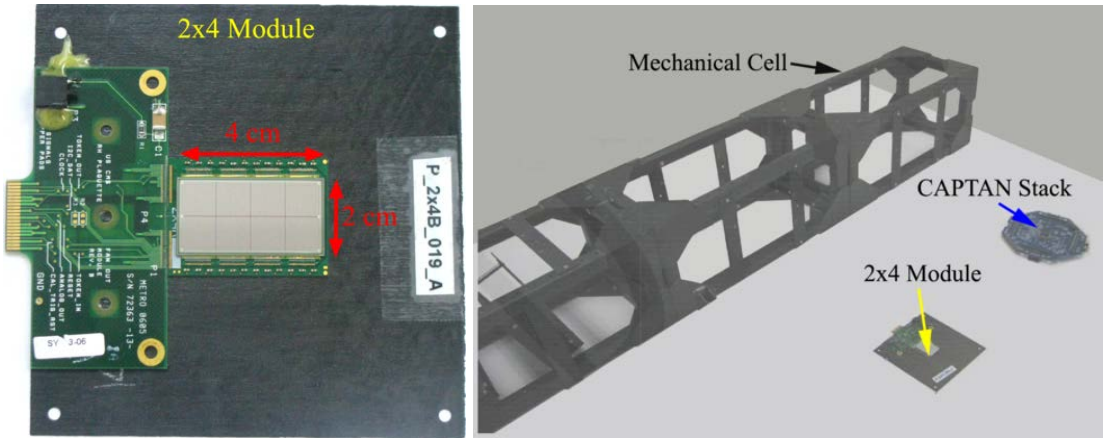

Figure 1. Left: CMS PSI46V2 module. Right: telescope mechanical structure together with its components.

Each ROC reads an array of 52x80 pixel cells, where each pixel cell is size 100 x 150 x 285 μm^3 (except for the pixels at the edge columns and upper row which have sizes 100 x 300 x 285 μm^3 and 200 x 150 x 285 μm^3, respectively), for a total square active area of 0.81 x 0.81 cm^2. The total active area for a 2x4 module is then 1.62 x 3.24 cm^2 while the 2x3 module total active area is 1.62 x 2.43 cm^2. The eight planes are arranged in two stations with a section available in between for the DUT. The DUT is considered a separate third station itself. The two telescope stations are identified by their position relative to the DUT: one placed upstream of the DUT station, with the other placed downstream of it. Each detector has a carbon fiber layer with the module glued on it. Heat is dissipated through the carbon fiber and hence no cooling is required. For each station, the detectors are grouped into two pairs and each pair of detectors is screwed together to a light aluminum mechanical support, then mounted on the mechanical structure of the telescope, as shown in Figure 2.

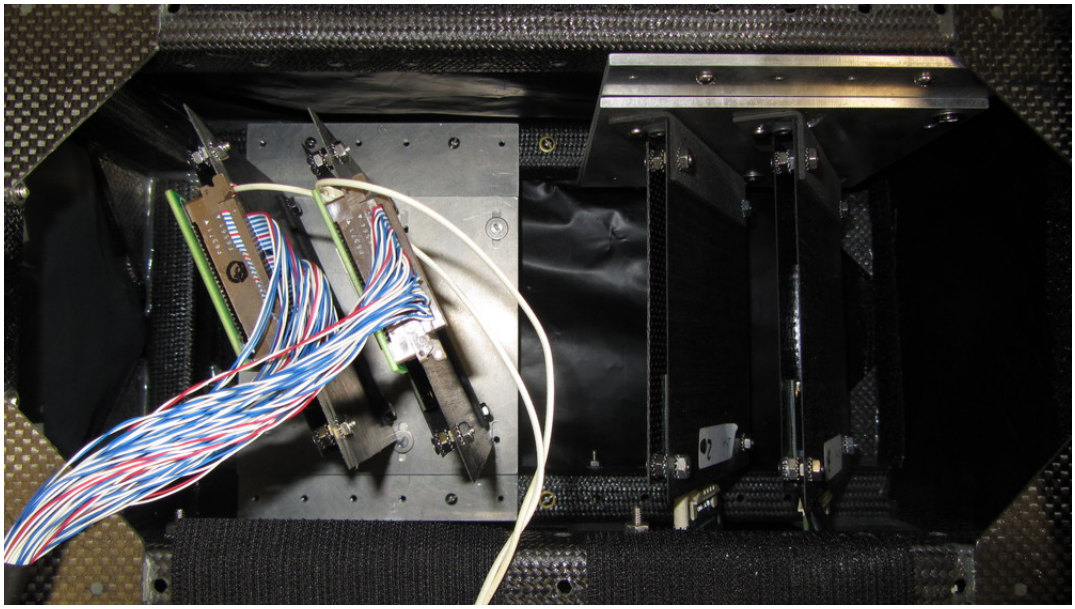

Figure 2. Modules mounted on the aluminum support at 25 degrees inside the carbon fiber frame.

The mechanical structure is of modular design: the telescope frame consists of three basic cells, one for each station, built with carbon fiber tubes of dimension 17.0 x 17.0 x 34.0 cm^3. The telescope frame is covered by a Mylar anti-static layer, as can be seen in Figure 3, which also serves the secondary purpose of keeping the detectors dark.

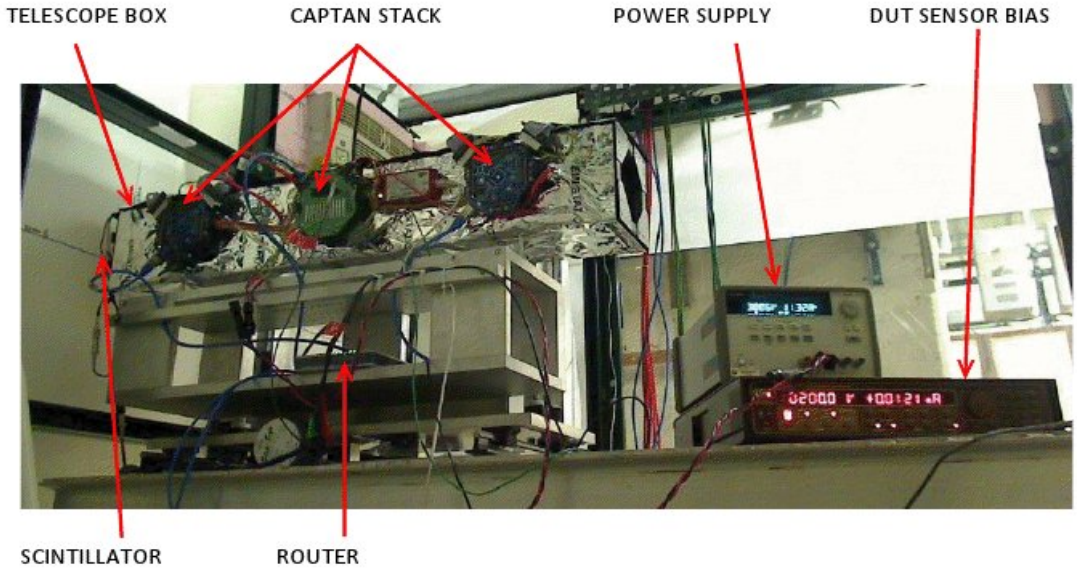

Figure 3. The CAPTAN pixel telescope complete assembly in situ at the FTBF.

A three-dimensional schematic view of the telescope detector planes is presented in Figure 4, where the laboratory coordinate system is also indicated. In this reference frame the Z axis is along the beam direction with +Z pointing downstream, the Y axis is perpendicular to the beam with +Y pointing upwards, and the X axis is the horizontal axis with +X given by the right-hand rule. The coordinate system origin is placed between the two stations so that each plane of upstream and downstream station has negative and positive Z coordinate, respectively.

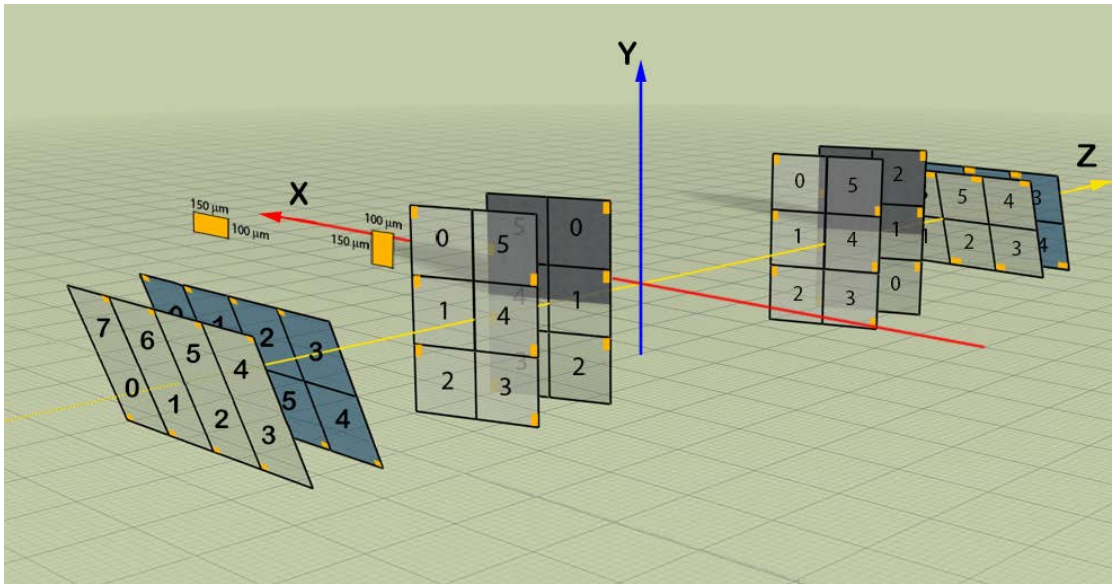

Figure 4. Three-dimensional schematic view of the pixel telescope.

In order to exploit the improvement in the spatial resolution when there is charge sharing between adjacent pixels, the planes are tilted by 25 degrees as follows:

- Four planes (2x4 detectors) tilted around the X axis with the long pixel side oriented in the X direction;
- Four planes (2x3 detectors) tilted around the Y axis with the long pixel side oriented in the Y direction.

In the first case, the most precise measurement is in the Y coordinate, while in the second case the most precise measurement is in the X coordinate. This geometry give a total overlap active area of ~ 1.6 x 1.6 cm^2.

Each particle spill is triggered by the coincidence signal of three scintillation counters placed behind the telescope. The trigger signal opens a small time window in which the data acquisition system collects and sends data from the detectors to the computer. The data from each ROC are tagged with the trigger count, so that data recorded from all the detectors has the same tag if they are correlated in time. The hits that share the same trigger count are identified as an event. An event may contain hit data associated with one or more particle tracks passing through the telescope.
To keep the ROCs synchronized with the particle beam, the accelerator clock signal is fed into one of the station and then redistributed to the other stations through SATA cables. Since the CMS ROC has been designed to run at a frequency of 40 MHz while the Main Injector accelerator frequency is 53 MHz, the clock that is distributed to the stations runs at 27 MHz, half of the Main Injector frequency, allowing the detector to work properly and still keeping it synchronous with the beam.

3 The Data Acquisition System

3.1 The DAQ: hardware

The Data Acquisition (DAQ) hardware is based on the CAPTAN system developed at Fermilab [3]. The CAPTAN (Compact And Programmable daTa Acquisition Node) is

a flexible and versatile data acquisition system designed to meet the readout and control demands of a variety of pixel and strip detectors for high energy physics applications.

The system is characterized by three key architectural features: a vertical bus that allows the user to stack multiple boards, a Gigabit Ethernet Link (GEL) that permits high speed communications to the system, and the core boards to provide specific capabilities for the system. The system is based on core elements known as system nodes. A node is a stack of boards connected together by the vertical bus. There are no limits to the number of nodes that can work together in a system; the only limit is for the number of boards that a vertical stack can contain (about ten) due to signal quality degradation. The CAPTAN architecture supports two types of data paths, namely, the intra-node and the inter-node data paths. The intra-node communication is achieved by means of the vertical bus that connects all the boards in the same node. The inter-node communications are realized by two different paths, the horizontal bus and the GEL.

Another key feature of the architecture is the existence of core or primary boards providing the backbone of the node system forming the central part of the hardware. Each of the two telescope stations has a CAPTAN node that consists of two octagonal primary boards (Figure 5):

- The Node Processing and Control Board (NPCB) provided with a Virtex-4 FPGA.
- The Data Conversion Board (DCB) provided with a 12-bit MAX1438 Analogue to Digital Converter.

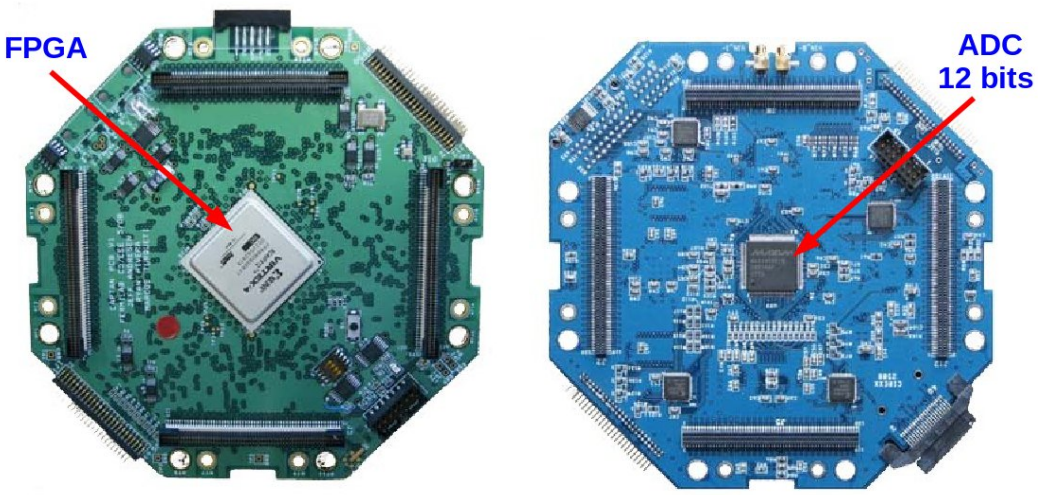

Figure 5. Pictures of the primary boards of the CAPTAN stack used for telescope data acquisition. Left: Node Processing and Control Board. Right: Data Conversion Board.

The two boards are stacked together as shown in Figure 6. Each NPCB is connected to a gigabit Ethernet router and the router is, in turn, connected to the computer placed in the FTBF control room through an Ethernet cable. This computer is where the graphical user interface, which controls the entire telescope system, runs.

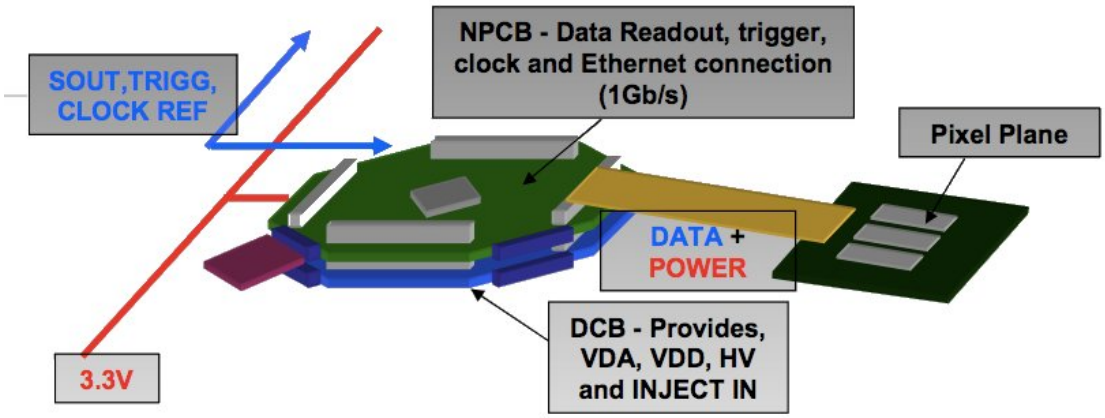

Figure 6. Depiction of the CAPTAN stack used for telescope data acquisition.

The trigger signal from the scintillation counters arrives over a LEMO cable to the NPCB of the central station node, called Master station, from which it is distributed over SATA cables to the outer station nodes. The Master station must then be present even in the absence of any DUT attached to it since it functions as a clock and trigger distribution node. The external Main Injector clock (53 MHz) for synchronization of the stations follows the same path after being reduced to half the frequency inside the FPGA of the Master station.
For each telescope station, the data from ROCs are received by the DCB, digitalized by the ADC, and then sent to the FPGA. The formatted data are then transferred to the control room PC via gigabit Ethernet. The diagram in Figure 7 shows the full readout system schematically.

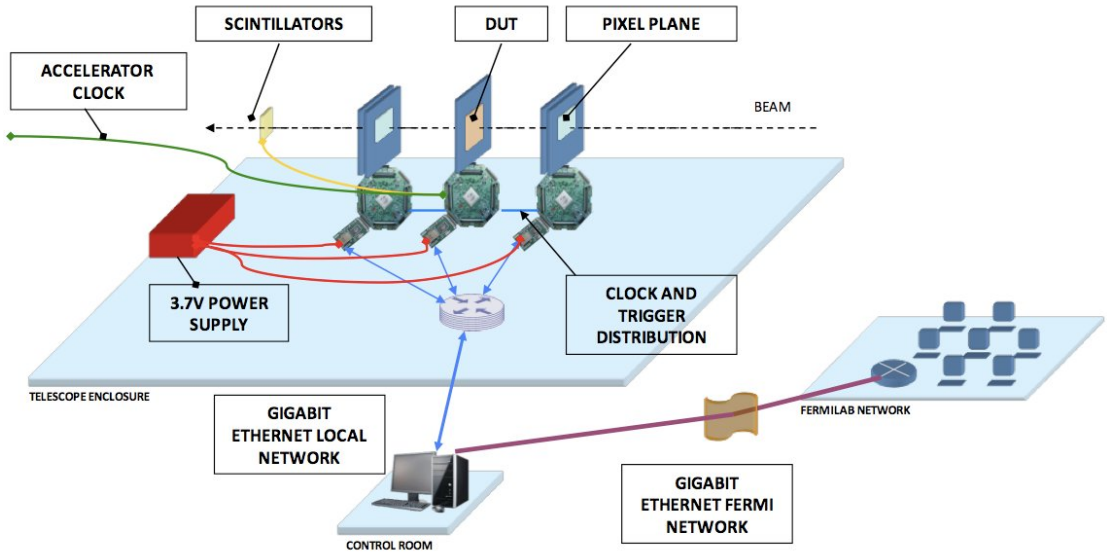

Figure 7. Schematic of the telescope readout system based on CAPTAN hardware.

At the control room PC, the data from each CAPTAN node are stored in separate directories. Within each directory, the runs are segmented into many partial-run files where the binary data resides. Files from different directories are then sequentially scanned and all temporally correlated data from every pixel plane (marked with the same the trigger count) are pulled from the file and merged to form what represents an

event. A single binary file containing the merged events is then created for each run. Each pixel data is stored in a 64 bits word (8 bytes), so the typical size of a raw data event with clusters made of two pixels hit on all eight planes is only about 128 bytes. The data saved on disk is the raw data coming from the CAPTAN station without any manipulation, thus the effective data rate from the detectors is of the order of ~ 12.8 Mbytes/sec for each of the 4.2 seconds of spill every minute at a particle rate of ~100 KHz. The gigabit Ethernet link handles this amount of data without any data loss and has been tested up to rates of ~150 KHz without any performance degradation.

3.2 The DAQ: software

A complete software solution for interfacing with the CAPTAN system has been designed for Microsoft Windows using Microsoft Visual C++ 2008 [4].

The diagram in Figure 8 shows the CAPTAN software topology schematically. The building blocks of the software are the Global Master (GM), the CAPTAN Controller (CC), a Graphical User Interface (GUI) and the CAPTAN Analysis and Display (CAD).

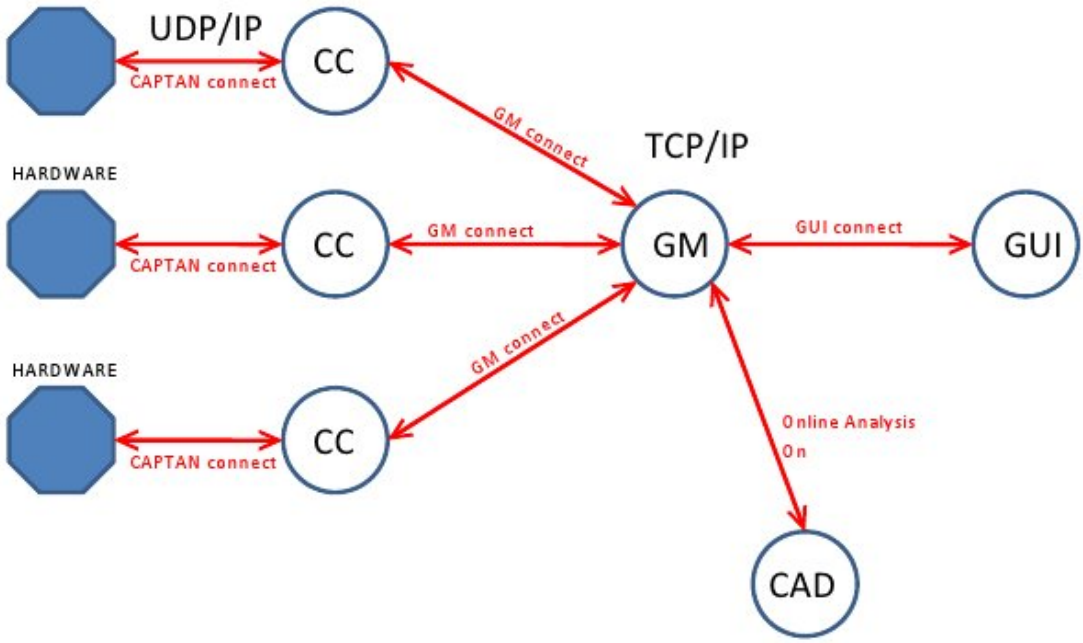

Figure 8. Schematic of the telescope readout system based on CAPTAN hardware.

The GM is the server for the entire system. It forwards commands from the user to the CAPTAN system and it sends data from the system to the user for interpretation. The CC provides the basic connection between a CAPTAN stack and the GM so that there is a CC for each of the three stations. The messages it receives from the GM destined for its CAPTAN stack are forwarded to that, and the data that is returned from the stack is either stored to disk or handed off to the GM for delivery to the GUI depending on the configuration. The GUI initiates all writes and reads to and from the CAPTAN. It allows the user to set up the readout chips, trigger and clock system, run calibration procedures, as well as to start or stop the data acquisition. It also controls when the CC stores data to disk. The final block of the software architecture is represented by the CAD that allows the user to immediately visualize the telescope merged data in three dimensions as shown in Figure 9.

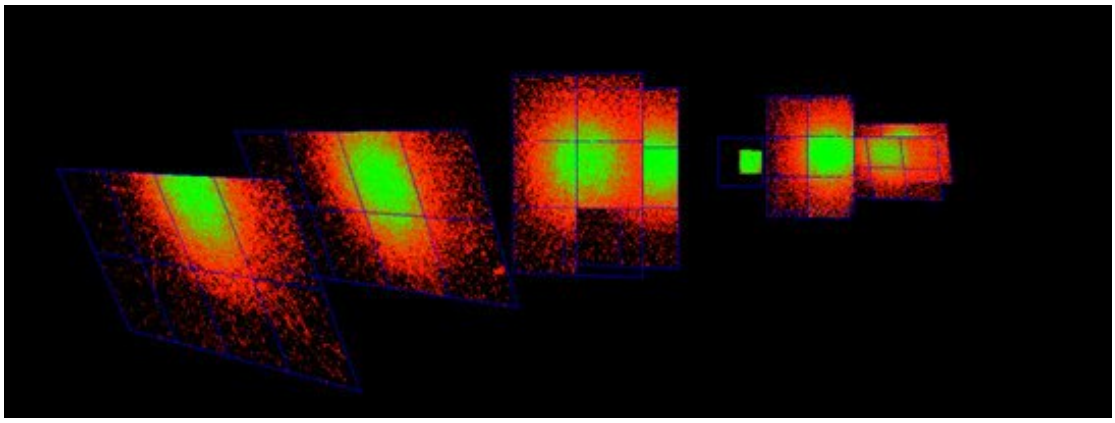

Figure 9. Three-dimensional data visualization with the CAPTAN software.

This is critical for the data acquisition process since it allows the user to quickly check the quality of the data. For instance, this feature makes it possible to recognize if the beam is positioned properly on the detectors. The telescope is seated on a X-Y motion table that can be controlled remotely from the control room and can be moved around in case the beam is not passing through the detectors. Figure 10 shows a picture of the various CAPTAN software blocks.

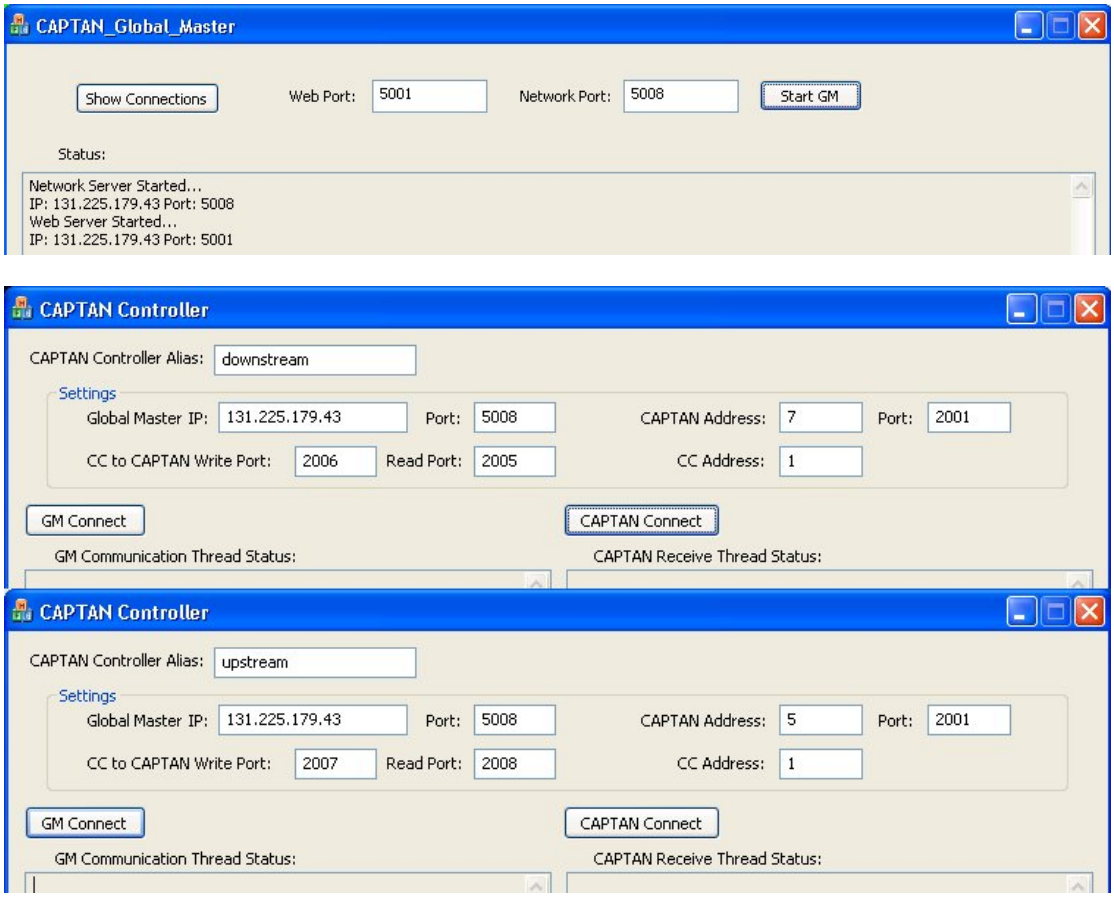

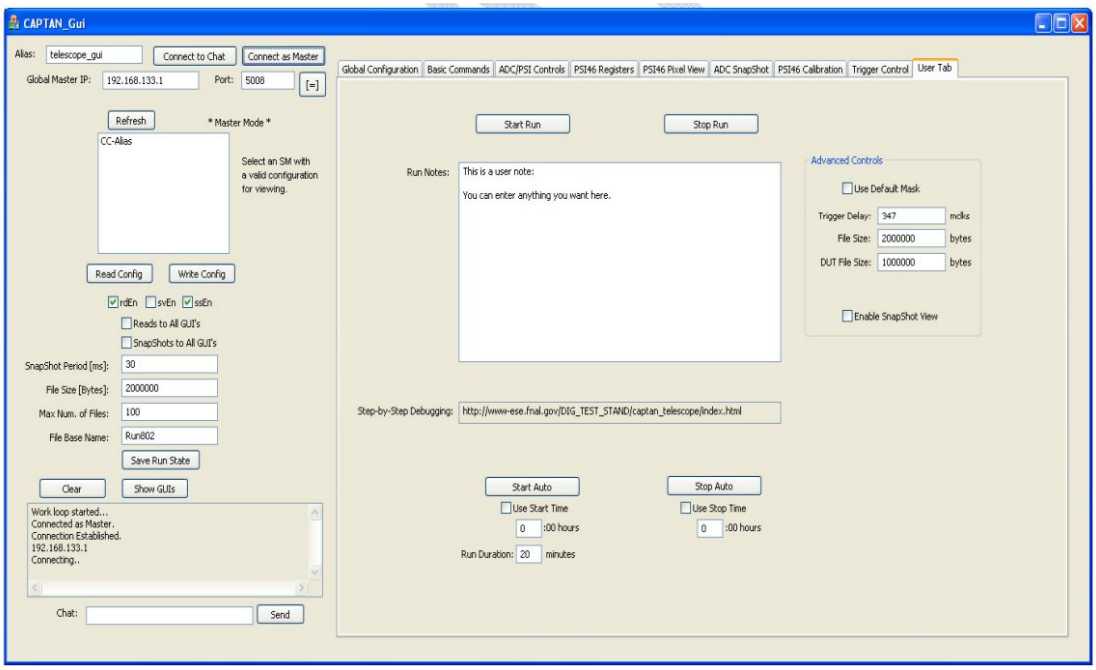

Figure 10. Screenshots of the CAPTAN software blocks.

4 Telescope Tracking and Alignment

The main goal of the test beam experiments is to probe the performance of the DUT with a set of well identified and reconstructed beam tracks. For this purpose the telescope has been designed to achieve an optimal resolution on the coordinates of the track impact point on the DUT, which is conveniently placed at the center of the telescope. The track reconstruction and the telescope alignment are performed by means of the C++ package Monicelli, developed by the INFN Milano-Bicocca group. This software package provides the user with an appropriate iterative procedure that should be guided to converge toward the right alignment. All the operations can be accomplished in steps through a graphical interface that makes the software user-friendly. Furthermore, each step of the procedure produces a number of distributions that allow monitoring its status and progress. The software is also equipped with efficient interactive tools allowing the user to browse, examine, print and save these distributions in real-time. Figure 11 shows a snapshot of the Graphical User Interface (GUI) and its components.

The next paragraphs give an overview of the main operations of the track reconstruction and iterative alignment procedure.

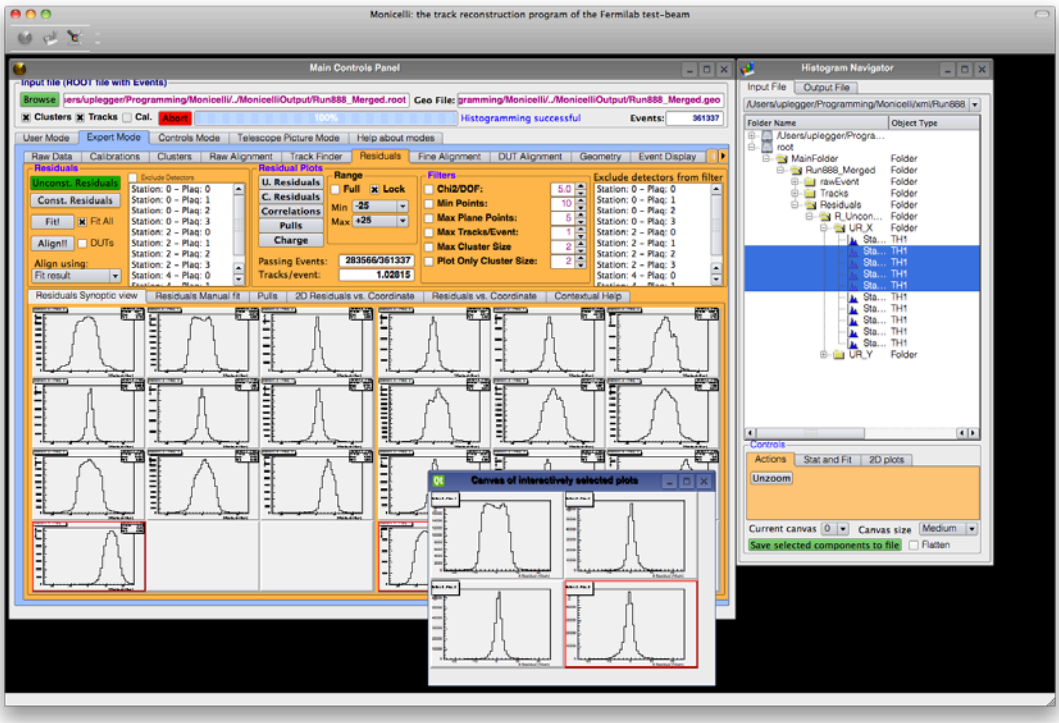

Figure 11. Monicelli Graphical User Interface. Inside the desktop style GUI, the main panel on the top left that controls all alignment operations is shown while on the right it is shown the histogram browser used to plot the control histograms created during the alignment phases. Histograms can be viewed inside the control panel and also in canvases, on the bottom, opened by the histogram browser.

4.1 Track Reconstruction

In the first step of the track reconstruction process, Monicelli reads the merged binary data file together with an XML geometry file describing the overall configuration and the geometrical details of the telescope detectors for that particular set of collected data. This file is editable by the user by means of an easy editor included in the package. The geometrical details of each plane are set specifying its space coordinates and rotation angles in the laboratory frame, as well as the number and orientation of ROCs and, for each ROC, the number of columns and rows together with their pitch.

In this stage the information contained in the binary file is decoded: for each event, the ADC value of every pixel hit is associated with the new row and a column value corresponding to the position on the detector according to the telescope information provided by the XML file. Two output files are created on disk: one with decoded events data and another with the associated geometry. In addition, the two-dimensional distribution of the hits accumulated by each pixel plane in that Run is generated as shown in Figure 12.

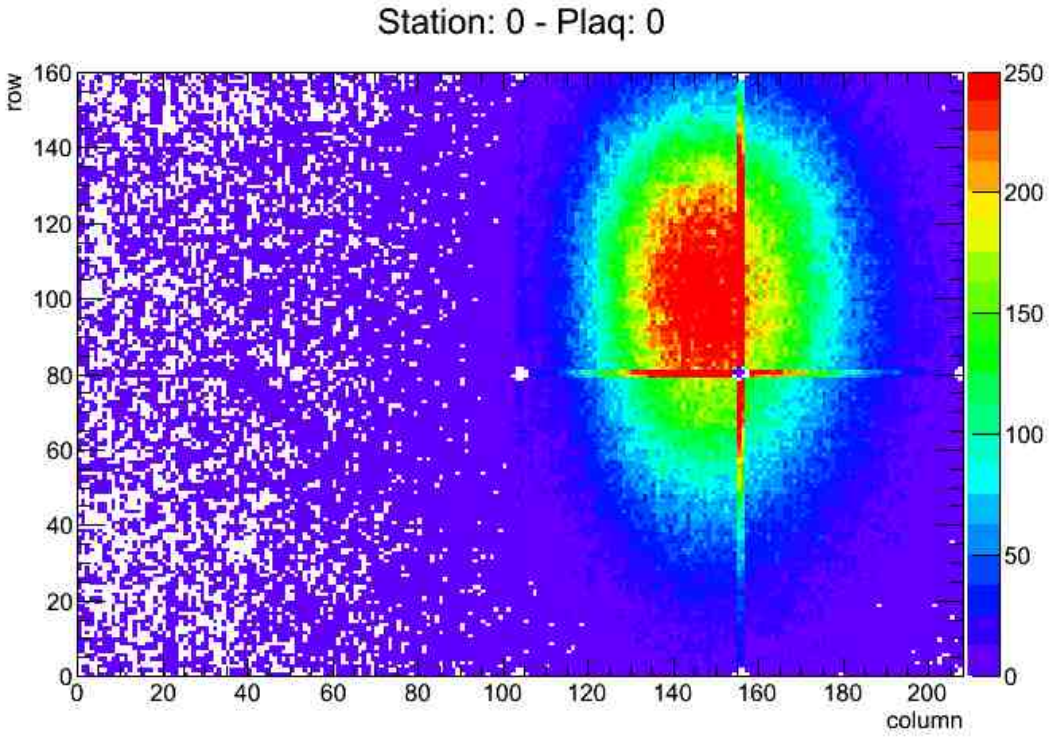

Figure 12. Beam spot on one of the telescope detectors

These histograms allow users to cross-check the geometry information provided to the program as well as check that the beam is roughly centered on all the detector planes.
The next step in the reconstruction process consists of finding the clusters of adjacent fired pixels in order to attribute to each of them the proper weighted coordinate. Only clusters of one pixel, two adjacent pixels on a row or a column and four adjacent pixels (2×2) are considered for track reconstruction. The other are not used because very rare and, in some cases, resulting from complex processes or detector pathologies, which do not allow for a reliable coordinate interpolation (two tracks, δ-rays, threshold cut, noisy or dead pixels, etc.).
The cluster coordinates are expressed as local coordinates (to distinguish them from the laboratory system coordinates X and Y as defined in Fig. 4) of the particular detector they belong to: the *x*-axis is, by definition, parallel to the pixel rows, the *y*-axis to the pixel columns.

For single hits, the coordinates are simply those of the pixel center:

$$x = x_c$$
$$y = y_c$$

For two adjacent hits on a column, the *y*-coordinate is linearly interpolated over the expected charge-sharing width, *W*, whereas x is that of two pixel centers, x_c. Depending on the angle α between the *y*-axis and the plane normal to the beam, *W* can range from a typically diffusive value of 20 μm ($\alpha \approx 0°$) to a geometry-dominated value of $t \times \tan\alpha$ ($\alpha > 10°$), where $t = 280$ μm is the thickness of the pixel sensor. In the intermediate region of α, the two charge-sharing mechanisms are comparable and, therefore, they should be properly combined. Since the present telescope features α angles, which could be approximately 25^{o} only, the resulting coordinates are:

$$x = x_c$$
$$y = y_d - \frac{W(25^o)}{2} + W(25^o)\frac{Q_L}{Q_L + Q_R}$$

where y_d is the coordinate of the divide of the two pixels, Q_L (Q_R) is the charge collected by the pixel on the left (on the right) and $W(25^o) = 130\mu m$.
Recalling that the angle β between the *x*-axis and the plane normal to the beam is $\approx 0^o$ for all planes of the telescope, the resulting coordinates for two adjacent hits on a row are:

$$x = x_d - \frac{W(0^o)}{2} + W(0^o)\frac{Q_L}{Q_L + Q_R}$$
$$y = y_c$$

where $W(0^o) = 20\mu m$.
The same argument can be extended to treat 2×2 clusters by defining

$$^xQ_L = Q_{i,j} + Q_{i+1,j}$$
$$^xQ_R = Q_{i,j+1} + Q_{i+1,j+1}$$

for *x*-interpolation, and

$$^yQ_L = Q_{i,j} + Q_{i,j+1}$$
$$^yQ_R = Q_{i+1,j} + Q_{i+1,j+1}$$

for *y*-interpolation; *i* and *j* are respectively the row and column index of the bottom-left pixel of the cluster. In this way, the coordinates given to a 2×2 cluster are

$$x = x_d - \frac{W(0^o)}{2} + W(0^o)\frac{^xQ_L}{^xQ_L + ^xQ_R}$$
$$y = y_d - \frac{W(25^o)}{2} + W(25^o)\frac{^yQ_L}{^yQ_L + ^yQ_R}$$

The errors associated with these cluster-coordinates were obtained directly from the data by requiring unit pulls of the track-hit residuals for each type of clusters (only reconstructed tracks with hits on all the telescope planes are considered). To this extent, an iterative procedure was set up: at each step of the procedure a better approximation of the errors was available to refit the tracks, to calculate the pulls and, eventually, to further refine the errors for the next step.
The measured errors are:

$$\sigma_x = \frac{150}{\sqrt{12}}\ \mu\text{m} = 43.3\ \mu\text{m}$$
$$\sigma_y = \frac{100\left(1 - \tan 25^o\right)}{\sqrt{12}}\ \mu\text{m} = 15.4\ \mu\text{m}$$

for single hits (recall $\beta \approx 0^o$),

$$\sigma_x = \frac{150}{\sqrt{12}}\ \mu\text{m} = 43.3\ \mu\text{m}$$
$$\sigma_y = 7.8\sqrt{1 + \tan^2 25^o}\ \mu\text{m} = 8.6\ \mu\text{m}$$

for two adjacent hits on a column, and

$$\sigma_x = 7.8\ \mu\text{m}$$
$$\sigma_y = \frac{100}{\sqrt{12}}\ \mu\text{m} = 28.9\ \mu\text{m}$$

for two adjacent hits on a row.
For 2×2 clusters the errors are assumed to be:

$$\sigma_x = 7.8\ \mu\text{m}$$
$$\sigma_y = 7.8\sqrt{1 + \tan^2 25^o}\ \mu\text{m} = 8.6\ \mu\text{m}$$

Once the clusters have been reconstructed, the next operation consists of finding track candidates. This is done trying to join with a straight line any combination of cluster hits on the first and the last plane of the telescope and looking for confirming hits on the intermediate planes. The nearest cluster hit to the intersection point of the line on every plane within an adjustable window is selected. A minimum of 6 hits is required to define a track candidate. Other track candidates can reuse the clusters during this operation. The hits associated to each track candidate are fitted to a straight line using the least square method. When all track candidates in an event are reconstructed and fitted, they are sorted by total number of hits and χ^2/DoF. For all the track candidates, starting from the track with the highest number of hits and the lowest χ^2/DoF, all hits belonging to the track, that have been associated to other track candidates, are removed from them and those tracks are refitted and resorted again.

4.2 Alignment Procedure

This paragraph describes the final strategy that has been successfully adopted to align telescope detectors with beam-test data. The alignment results obtained with Monicelli will be subsequently discussed in the last section.

1. The alignment requires an initial set of track candidates to start with. In turn, this implies that a preliminary raw alignment of the telescope detectors has to be performed. This first-order approximation is obtained in Monicelli by a relative

transverse alignment of the beam profiles on each detector. To this extent, the X and Y projections of the beam spot are fitted with a Gaussian function to obtain the space coordinates of the beam spot centers on each telescope detector.

2. An initial suitable sample of tracks is then found through a “road search", as described in the previous section, performed with large enough window tolerances (usually 1000 μm) and without any other cuts.
3. A finer translation alignment is obtained by looking at the mean values of the X and Y residuals on each plane (at this stage they are typically off from zero by a few hundred microns). At the end of this operation, the X and Y detector positions in the geometry file are automatically updated with the measured translation corrections.
4. A new “road search" is now performed with a narrower window (usually 250 μm wide) and a better sample of tracks is obtained as indicated by the χ^2/DoF distribution whose peak is reduced to well below 20.
5. At this stage some additional cuts are applied for a further “road search", requiring for instance
   - χ^2/DoF < 20
   - 8 hits per track
   - no more than 1 hit per plane

   A further look at X and Y residual distributions will give, at this stage, a residual detector translation of a few microns in both directions and the core of the χ^2/DoF distribution well below 10.
6. Step 3 can be iterated to find a better sample of tracks candidates.
7. At this stage, alignment conditions are ready to proceed with the fine alignment iterative algorithm that exploits a least-squares minimization to compute the 1st-order roto-translational corrections. A sample made of tracks with 8 hits, each of maximum cluster-size 2, is selected to compute and minimize the *x* and *y* (*local coordinates*) unconstrained residuals on each telescope detector. In this first iterative minimization run, the geometry parameters of the first and the last detector along Z direction are kept fixed. Furthermore, if the angular dispersion of the beam tracks is tiny (≈ .1 mrad), even the Z positions of the other detectors have to be fixed since the fit would be insensitive to any shift in Z (the derivatives of χ^2 with respect to these Z positions would practically be zero). At the end of each iteration, a new “road search" is performed with the updates to provide the next iteration with an improved sample of tracks. Typically, 5 iterations are enough to converge to stable values of the parameters. The number of iterations can be set by the user (10 iterations by default) as well as the χ^2/DoF cut (χ^2/DoF < 10 by default). At the end of this process, pull, unconstrained residual and correlation distributions are produced to check the alignment progress.
8. Finally, a second iterative minimization run is executed releasing also the geometry parameters of the first and last planes while keeping fixed the Z positions of all the telescope planes. Usually, as for step 7, 10 iterations are set with a χ^2/DoF cut of 10. The resulting updated parameters constitute the final alignment geometry.

4.3 Alignment Results

Applying the previously outlined alignment procedure, convergence has been reached for all the test beam data with the present telescope. An example of the final result is given in this section for a particular data Run. The following distributions have been created for a sample of tracks satisfying some requirements:

- χ^2/DoF < 10
- 8 hits per track
- no more than 1 hit per plane
- a maximum hit cluster-size of 2

Figure 13 shows the *x* and *y* unconstrained residual distributions (*local coordinates*) after a complete alignment for one of the telescope planes. The unconstrained residuals are defined on each detector as the difference between the coordinates of the measured hit and those of the impact point of the track fit obtained excluding that particular hit. As shown in the figure, the residual spectra show both a larger non-Gaussian shape along the non-tilted coordinate (pitch = 150 μm) and a narrow shape along the tilted one (pitch = 100 μm). The former shape is caused by the most probable single-hit events, resulting in distributions with RMS of about 150/√12. In the second case the distribution is dominated by charge sharing between adjacent pixels along the coordinate that is measured with the best resolution, resulting in distributions with RMS of about 24 μm.

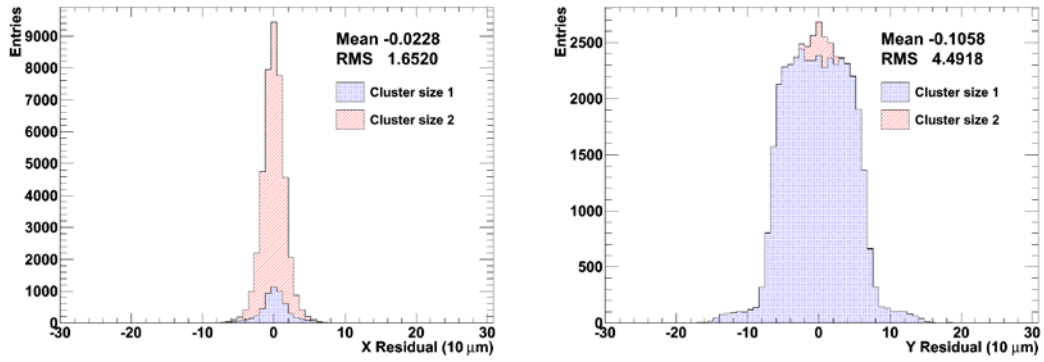

Figure 13. The *x* and *y* residual distributions for one telescope detector after a complete alignment

Figure 14 shows the *x* and *y* pull distributions after a complete alignment for one of the telescope detector. The pull ($p_{x,i}$, $p_{y,i}$) on a detector *i* is defined as the unconstrained residual normalized to its error, i.e. the square-root of the sum in quadrature of the error associated to the measured hit coordinates ($x_{m,i}$, $y_{m,i}$) and the error on the impact point ($x_{p,i}$, $y_{p,i}$) of the track fit obtained excluding the hit on that plane:

$$p_{x,i} = \frac{x_{m,i} - x_{p,i}}{\sqrt{\sigma^2_{x_{m,i}} + \sigma^2_{x_{p,i}}}} \;,\; p_{y,i} = \frac{y_{m,i} - y_{p,i}}{\sqrt{\sigma^2_{y_{m,i}} + \sigma^2_{y_{p,i}}}}$$

The quasi unitarity of the *x* and *y* pull distributions confirms the correct estimate for the different hit resolutions.

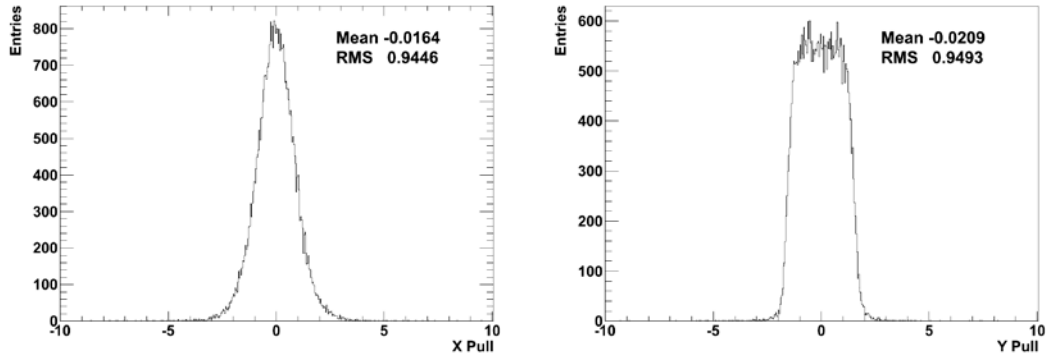

Figure 14. The *x* and *y* pull distributions for one of the telescope detectors

The accuracy of the alignment is further investigated studying the plots of Figure 15, showing the correlations between the unconstrained residuals and the impact point coordinates on the detector. Any deviation from a flat distribution would signal a residual problem in the alignment. As the alignment procedure goes ahead, the correlation plots are flattened and become as those shown in the figure.

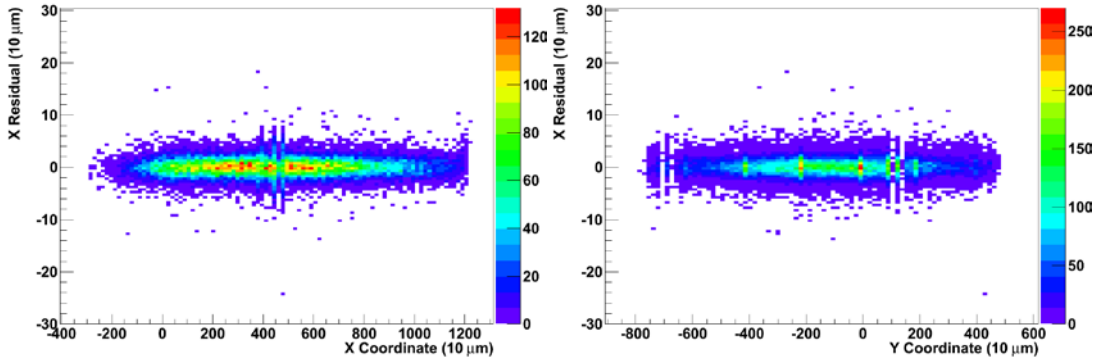

Figure 15. Plots of the correlation between unconstrained residuals and impact point coordinate for one of the telescope detectors.

The shape of the fitted track χ^2/DoF distribution in Figure 16 shows the quality of the tracks reconstructed with this alignment, highlighting the efficiency of the alignment procedure.

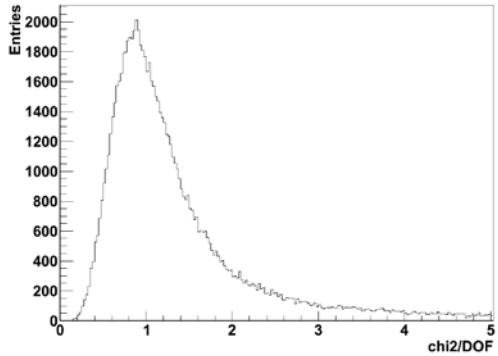

Figure 16. The track χ^2/DoF distribution after a complete alignment.

Figure 17 reports the X and Y slope distributions of the 120 GeV proton tracks

showing a very small angular dispersion (~10^{-4} rad), which results in a low resolving power for the determination of Z position corrections.

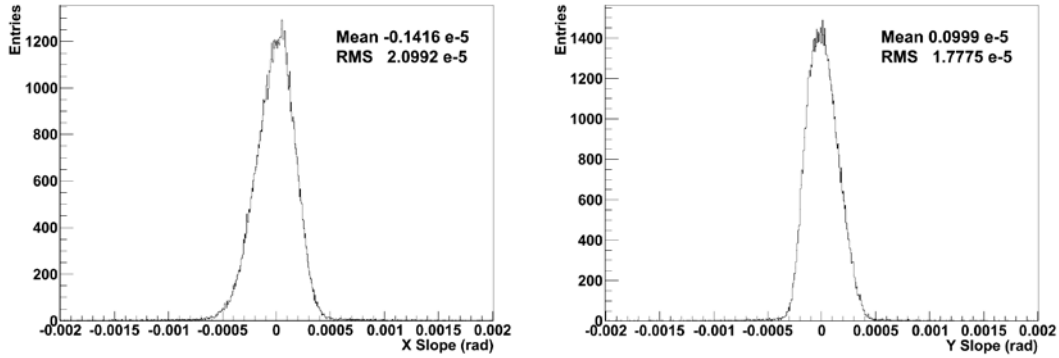

Figure 17. The slope distributions of the 120 GeV proton tracks.

Finally, the transverse error on track fit extrapolation at DUT Z position (Z≈0) is plotted in Figure 18 for tracks with 8 hits. It turns out that the best achievable telescope resolutions on the DUT is as small as 5.5 μm in both X and Y coordinates, and that the bulk of tracks give resolutions better than 7 μm.

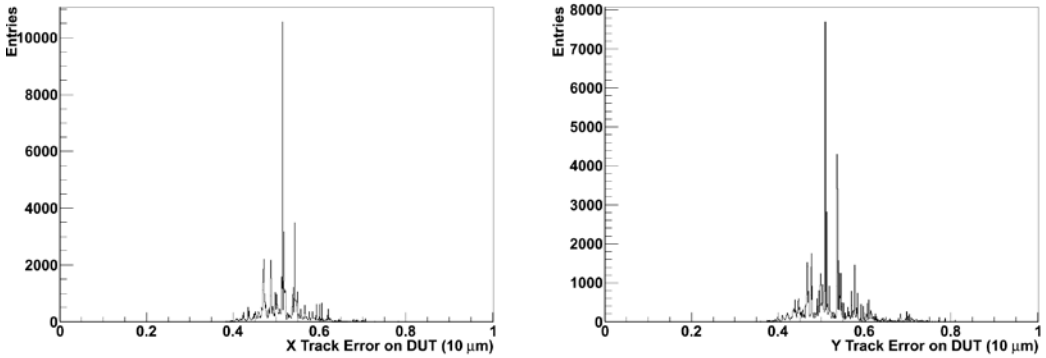

Figure 18. Track fit extrapolated error distributions at the DUT Z position (Z = 0) after a complete alignment. The discrete peaks result from the combinations of different hit resolution that can be associated to the tracks.

5 Conclusions

This paper describes the pixel silicon telescope installed at the Fermilab Test Beam Facility (FTBF) that provides high resolution tracking of the beam particles. The impact point of the available 120 GeV beam protons at the center of the telescope can be reconstructed with an accuracy of about 6 μm on both the transversal coordinates. The detector hardware and control software is complemented by the Monicelli software, which provides to the users the reconstructed tracks necessary for their data analysis. The telescope has been already used by several experiments and, in particular, has been extensively used by the CMS forward pixel community to test sensor candidates for future CMS pixel upgrades.

Acknowledgements

We wish to thank the Fermilab Test Beam Facility personnel, and in particular Aria Soha, for the continuous support they provide us. This research was supported, in part, by the U.S. Department of Energy and the Italian Istituto Nazionale di Fisica Nucleare and Ministero della Ricerca Scientifica e Tecnologica.
We also wish to thank the LHC Physics Center (LPC) for the support given to our students Stefano Terzo, Jennifer Ngadiuba and Luigi Vigani.

Bibliography

[1] Fermilab Test Beam Facility web site: http://www-ppd.fnal.gov/FTBF
[2] H. Chr. Kaestli et al.: Design and Performance of the CMS Pixel Detector Readout Chip. Nucl.Instrum.Meth. A565 (2006) 188-194
[3] Marcos Turqueti, Ryan A. Rivera, Alan Prosser, Jeffry Andresen, and John Chramowicz. CAPTAN: A hardware architecture for integrated data acquisition, control, and analysis for detector development. In Nuclear Science Symposium Conference Record, 2008. NSS '08. IEEE, pages 3546-3552.
[4] Ryan A. Rivera, Marcos Turqueti, and Alan Prosser. A software solution for the control, acquisition, and storage of CAPTAN network topologies. In Nuclear Science Symposium Conference Record, 2008. NSS '08. IEEE, pages 805-808.